TELKOMNIKA, Vol.15, No.3, September 2017, pp. 1012~1021
ISSN: 1693-6930, accredited **A** by DIKTI, Decree No: 58/DIKTI/Kep/2013
DOI: 10.12928/TELKOMNIKA.v15i3.5737

Noise Analysis in VLC Optical Link based Discrette OP-AMP Trans-impedance Amplifier (TIA)

Syifaul Fuada*[1], Trio Adiono[2], Angga Pratama Putra[3], Yulian Aska[4]
Microelectronic Center, Institut Teknologi Bandung (ITB),
Jl. Tamansari No 126, Bandung (40132), West Java, Indonesia/ Telp: +62-22-2506280/
Corresponding author, e-mail: syifaulfuada@pme.itb.ac.id*[1], tadiono@stei.itb.ac.id[2],
anggapp@pme.itb.ac.id[3], yulian.ska@pme.itb.ac.id[4]

Abstract.
To design Visible Light Communication (VLC) system, there are several requirements that need to be met. One of the requirements is an active component selection (e.g. Op-Amp). As an ideal communication system, the VLC system has to be able to provide wide bandwidth access with minimum noise. The Transimpedance amplifiers (TIAs) is one of the main components in the optical system which is placed in the first stage of the receiver system. It is used to convert the current output from photodiode to voltage. We have designed a 1 MHz fGBW TIA with low noise (in µVrms range). This paper aims to explain the design and implementation of TIA circuit with photovoltaic topology which covers empirical calculations and simulation of TIA's bandwidth and its noise sources, i.e. resistor feedback noise, current noise, voltage noise and total noise based on RSS. The OP-AMP is chosen from Texas Instruments product, OPA380, and the photodiode is chosen from OSRAM, SFH213, then simulated by TINA-TI SPICE® software. The noise in TIA circuit is analyzed clearly. The developer kit is ready to be implemented in VLC system.

Keywords: *Transimpedance Amplifier, Visible Light Communication, Bandwidth, Noise*

1. INTRODUCTION

Visible Light Communication (VLC) is an alternative communication technology which has high potential to be implemented en masse in the future, because it can offer several advantages such as license free, wide bandwidth, low cost because its component device already commercially available (*e.g.* LED lamp), harmless for human eyes as long as its follow the standards and free from electromagnetic interference. VLC technology commercialization already begins from 2015. Several companies/institutions that developing VLC technology are Nakagawa Laboratories (Japan) [1], Disney research (Switzerland) [2], pureLifi Ltd (UK) [3], IMDEA Network Institute (Spain) [4], and much more. Besides that, many universities also provide laboratory access for VLC technology research, for example: Institut Teknologi Bandung (Indonesia) with research [5-17], Pukyong National University (South Korea) with research [18-19], Edinburgh University (UK) with research [20-21], National University of Singapore (Singapore) collaboration with Nanjing University (China) with research [22], Chulalongkorn University, Thailand [23], Kookmin University (South Korea) with KUET (Bangladesh) [24], etc.

VLC application for indoor environment, such as laboratories, offices, closed public places, homes, hospital and convention center, needs to be able to provide wide bandwidth to be accessed by multiuser. Visible light, theoretically has a large bandwidth (more than radio frequency, infra-red and laser communication), but the bottleneck is the limited bandwidth of the main component device, that is LED as a transmitter device and photodiode as a receiver device. Commercially available LED and photodiode which has large bandwidth are very expensive. The solution of this problem is by implementing modulation scheme which can optimize component limitation to obtain high-speed data transfer [25], besides that, equalization [26], MIMO scheme, and other techniques are also implemented. On the other side, LED is also a non-linear device which can affect performances of multi-carrier modulation such as OFDM.

Other than "bandwidth" and "non-linearity effect", another serious problem in VLC which can reduce its performance is "noise" from external and internal [27] source. The external noise caused by ambient light, such as from incandescent, fluorescent, flashlight and sunlight. The external light source with high intensity can cause the LED transmitted signal wrongly

Received April 8, 2017; Revised July 18, 2017; Accepted August 3, 2017

recognized by the photodiode because it is hard to be distinguished [28]. For the internal noise source, it is caused by the components which is known as *Johnson noise, flicker noise* and *shot noise.* Both of these noise sources can really disturb the data transfer if not minimized

The target of this research is to design the TIA circuit for VLC platform. Thus, the received signal in the receiver can be processed with low error and correctly. In the previous research, noise on the trans-impedance amplifier (TIA) domain has already been explained [29] but the explanation is only limited on the analytical calculus based on the article [30]. In this paper, the noise profile of the same domain (*i.e.* TIA) will be discussed but the discussion will also encompass the current noise, voltage noise, feedback resistor noise and the accumulation of the total noise using TINA™ simulator. This software is an open-source simulator which is provided by the Texas Instrument that provides tools to simulate the noise profile of the TIA circuit. Optical illustration of the link structure based VLC based on [30] is shown in Figure 1, where there is three internal noise source which exists on the TIA circuit.

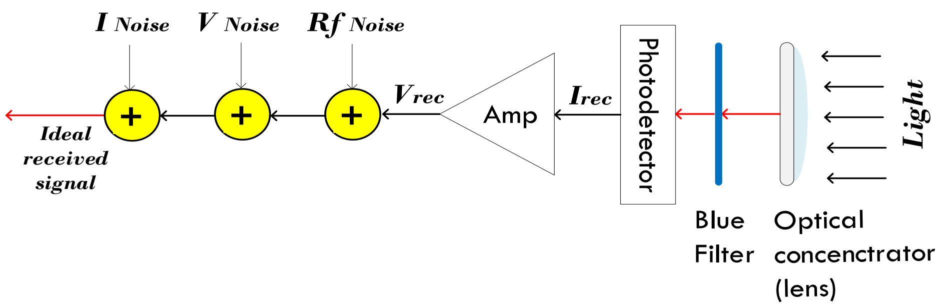

Figure 1. Analog Front-End Receiver in VLC Link based TIA

This paper is dedicated to discussing the noise of the discrete component based TIA circuit which uses one photodiode and one Op-Amp IC. The explanation approach is done by using the mathematical calculation and tools based simulation. This paper is divided into four main parts. The first part, discuss the background, which covers the explanation of the VLC technology, research development and several problems of the VLC system. The second part, cover the methodology of this research which also encompasses the component selection. The third part contains mathematical calculation and simulation results and analysis of the experiments. And the last part contains the conclusions, acknowledgments and references of this paper.

2. RESEARCH METHOD

The procedure of this research is, 1) equivalent modelling of the TIA circuit which shown in Figure 2, in this research we use photovoltaic mode topology of TIA which is a general topology for precision instrument application and generate low dark noise; Then 2) component selection for simulation, which is Op-Amp IC and photodiode as shown in Table 3 and 4; After that 3) listing the parameter characteristic of the circuit: *voltage noise density* (e_n), *current noise density* (i_n), *capacitor input* (C_{in}) and *capacitor junction* (C_j); 4) calculates Op-Amp capabilities; 5) calculates feedback resistor (R_f); 6) calculates feedback capacitor (C_f) and TIA noise; 7) plot the calculation results using *Kaleida V4.0* and 8) simulate using TINA, this software is really helpful in analyzing the circuit, it is easy to use and opened source from the Texas Instruments. It contains the library for many component selections of the Op-Amp types which ready to be used.

The OPA380 is an IC for TIA to be used for precision and high-speed application. It has low bias current (maximum of 50pA), wide bandwidth (around 90 MHz), so it is suitable to be used in the high-speed VLC application. The application of this IC model, in general, is for I/V conversion and photodiode monitoring. It has characteristics of low i_n (10 fA/√Hz) and low C_{in} (1.1 pF) also low e_n (5.8 nV/√Hz). For the photodiode, we choose SFH213 from OSRAM Opto semiconductors, which is a Si PIN photodiode. Its typical application is for high-speed photo interrupters. Its main capability is its fast switching time (5ns) and high short circuit current (I_{sc}), *i.e.* 125μA.

Table 1. The main characteristics of the IC Op Amp OPA 380 from Texas Instrument

Model	Open loop gain (dB)	voltage noise density (nV/√Hz)	current noise density (fA/√Hz)	Input bias current (pA)	Unity gain bandwidth (MHz)	Input capacitance (pF)
OPA 380	110	5.8	10	3	90	1.1

Table 2. The main characteristics of the Photodiode SFH213 from OSRAM Opto semiconductor

Model	Cj (pF)	Photosensitive area (mm)	Short circuit current (μA)	Rise time (μs)	Dark current (nA)	Noise equivalent Power (NEP)
SFH213	11	1 x 1	125	0.005	1	0.028 pW/$\sqrt{Hz}$

3. RESULTS AND ANALYSIS

3.1. Op-Amp capabilities calculation

In this case, the photodiode was modeled as light sensor in which the current source is in paralel with a capacitor junction (C_j). Based on *ac* signal analysis, the current source was open (ignored). So, C_j and R_s is in series combination. The value of C_j is given from the photodiode's datashet = 11pF, however the resistance is not shown. Therefore, we assume R_s = 100KΩ. The model of photodiode's output impedance is using Equation 1 where the calculation results is converted from rectangular to polar.

$$Z_{eq} = Z_{Rs} + Z_{Cj} = R_S + \frac{1}{sC_j} = R_S + \frac{1}{j\omega C_j}$$
$$Z_{eq} = \frac{1 + j\omega C_j R_S}{j\omega C_j} \quad (1)$$

Then the output impedance of the photodiode's model at the low frequency such as 1 kHz is calculated as:

$$Z_{eq} = \frac{1 + j\omega C_j R_S}{j\omega C_j} = \frac{1 + j2\pi * (1*10^3 Hz)(11*10^{-12} F)(10*10^3 \Omega)}{j2\pi * (1*10^3 Hz)(11*10^{-12} F)(10*10^3 \Omega)} = 0.14469\, M\Omega \angle -89.604^o$$

Then at the high frequency such as at 10 MHz, the impedance of photodiode is calculated as:

$$Z_{eq} = \frac{1 + j\omega C_j R_S}{j\omega C_j} = \frac{1 + j2\pi * (10*10^6 Hz)(11*10^{-12} F)(10*10^3 \Omega)}{j2\pi * (10*10^6 Hz)(11*10^{-12} F)(10*10^3 \Omega)} = 100\Omega \angle -0.829^o$$

Based on the calculation results, it can be seen that the higher the frequency, the impedance will fall. Based on **[31]**, "*at high frequency, the capacitor behaves as a short circuit and all the current will go through this path instead of the resistor path, creating a virtual short circuit, thus the impedance becomes much lower at high frequency"*.

In this case, the Op-Amp is modeled as a current source in parallel combination with a capacitor (C_{in}) as well as a resistor (R_{in}). The OPA380 has a very high input impedance of 10.000 GΩ/3 pF. The model of Op-Amp output impedance is using Eq. 2 where the calculation results are converted from rectangular to polar.

$$\frac{1}{Z_{eq}} = \frac{1}{Z_{Rs}} + \frac{1}{Z_{Cj}} = \frac{1}{R_S} + \frac{1}{\frac{1}{sC_j}} = + \frac{1 + j\omega C_j R_S}{R_S}$$
$$Z_{eq} = \frac{R_S}{1 + j\omega C_j R_S} \quad (2)$$

Then the output impedance of the Op-Amp model at the low frequency such as 1 kHz is calculated as:

$$Z_{eq} = \frac{R_S}{1 + j\omega C_j R_S} = \frac{(1*10^{13}\Omega)}{1 + j2\pi*(1*10^3 Hz)(3*10^{-12} F)(1*10^{13}\Omega)} = 53\,G\Omega \angle -89.999^o$$

Then at the high frequency such as at 10 MHz, the impedance is calculated as:

$$Z_{eq} = \frac{R_S}{1 + j\omega C_j R_S} = \frac{(10*10^{13}\Omega)}{1 + j2\pi*(10*10^6 Hz)(3*10^{-12} F)(10*10^{13}\Omega)} = 5.3\,K\Omega \angle -89.999^o$$

To obtain the input voltage of the TIA circuit, in this case, the current source substituted as a voltage source. Based on Figure 2, it can be known that input voltage on the (-) pin of Op-Amp can be modeled as voltage division of R_{in} and R_s, and can be expressed as Vs = V_{in} * (R_{in} / (R_{in} + R_s)). Then, the total impedance of the TIA circuit, if we ignore the capacitance component, is = $\frac{Z_{in}}{Z_{in} + Z_s}$. By using this equation, the input impedance of the SFH213 and the OPA380 can be calculated with taken magnitude component only. At the low frequency (10 kHz), the impedance is,

$$\frac{Z_{in}}{Z_{in} + Z_s} = \frac{53*10^9\ \Omega}{0.14469*10^6\Omega + 53*10^9\ \Omega} = 0.9999$$

At the high frequency (10 MHz),

$$\frac{Z_{in}}{Z_{in} + Z_s} = \frac{5.3*10^3\ \Omega}{100\,\Omega + 5.3*10^3\ \Omega} = 0.9814$$

The difference between both of the above calculation is around 0.01, relative small than in the frequency range of 10 kHz to 10 MHz. This shows that, at low and high frequencies, the input impedance of the OPA380 is much higher than the impedance of the photodiode. Using this mathematical model, the TIA circuit can be used to convert a high impedance signal to a low impedance signal.

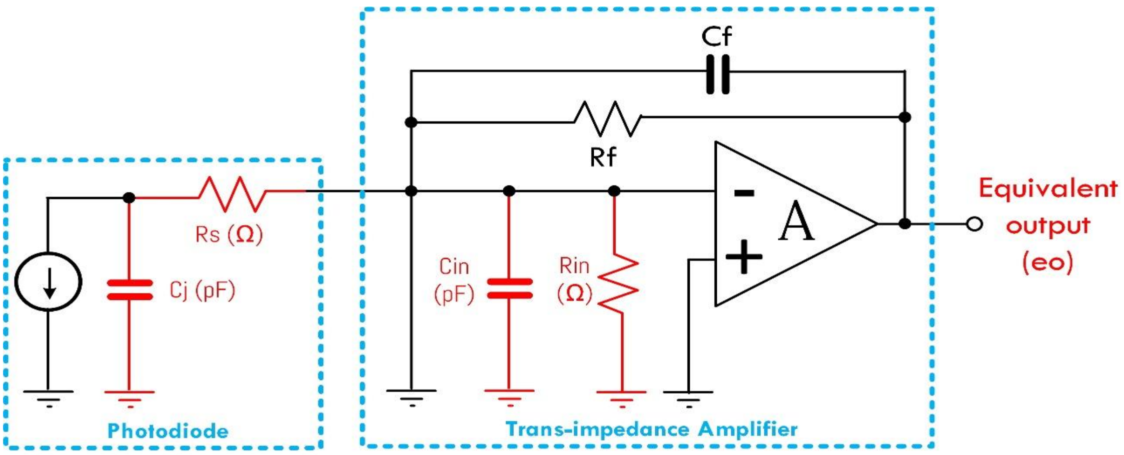

Figure 2. The equivalent circuit of TIA

3.2. Resistor Feedback, Capacitor Feedback and Bandwidth calculation

The photodiode as receiver component in VLC system, receiving information signal that is transmitted from LED which linear with illumination level, the higher the illumination level the generated current in the photodiode will become higher. This current then converted into the voltage by the TIA circuit. To put it simply, TIA circuit can be made from discrete components with one Op-Amp and two passive components (resistor and capacitor). The Resistor is used to determine the gain and capacitor is used to reduce the noise. According to Table 2, photodiode will generate current of 125µA, and TIA output voltage target is 1 V_{DC}. Referencing from Eq. 4, the chosen R_f value is 8 kΩ. Then the calculation of C_f (with 45^o of phase margin) is shown in Eq. 5, where C_{in} is Op-Amp input capacitance in Farad (see value in Table 1) and C_j is photodiode's shunt capacitance in Farad (see value in Table 2). The desired bandwidth (gain-bandwidth product or GBW) is 1 MHz. Afterward, the cut-off frequency (f_{-3db}) from the TIA circuit can be obtained using Eq. 6.

$$R_f = \frac{V_{out}\text{target}}{I_{SC}} = \frac{1\,V}{125\,\mu A} = 8\,k\Omega \tag{4}$$

**available = 8.2 kΩ*

$$C_f = \sqrt{\frac{C_J + C_{in}}{2\pi * R_f * f_{GBW}}} \tag{5}$$

$$C_f = \sqrt{\frac{11pF + 1.1pF}{2\pi * 8K * 1MHz}} = 15.52\,pF$$

**available = 15 pF or 22 pF*

$$f_{-3dB} = \sqrt{\frac{f_{GBW}}{2\pi * R_f * (C_{in} + C_j)}} \tag{6}$$

$$f_{-3dB} = \sqrt{\frac{1MHz}{2\pi * 8k * (1.1pF + 11pF)}} = 1.28\,MHz$$

3.3. Noise Calculation

In this paper, we analyze the noise in TIA circuit based on the root mean square (RMS) from the three noise sources, *i.e.* current noise, voltage noise and R_f noise. Calculation *Equivalent of noise bandwidth* (ENBW) can be done using Eq. 7.

$$ENBW = f_{-3db} * \frac{\pi}{2} \tag{7}$$

$$ENBW = 1.28\,MHz * \frac{\pi}{2} = 2.01\,MHz$$

After the ENBW is known, the next step is calculating the R_f noise of the TIA circuit which can be done using Eq. 8. Where *T* is the temperature with 283 Kelvin and *k* is the Boltzmann constant which is 1.38 × 10^{-23}.

$$N_{Rf} = \sqrt{4kT * ENBW * Rf} \tag{8}$$

$$N_{Rf} = \sqrt{4 * \left(1.38 * 10^{-23} \frac{m^2 kg}{s^2 K}\right) * 298K * 2.01\,MHz * 8K\Omega} = 16.28\,\mu Vrms$$

Then the current noise will appear on the Op-Amp's output after going through the R_f, it can be calculated using Eq. 9 where the I_n variable is the *current noise density*. The voltage noise calculation is based on Eq. 10,

$$N_{current} = I_n * R_f * \sqrt{ENBW} \quad (9)$$

$$N_{current} = 10\frac{fA}{\sqrt{Hz}} * 8K * \sqrt{2.01\,MHz} = 0.11\,\mu Vrms$$

$$N_{Voltage} = e_n\left(\frac{C_{in} + C_j + C_f}{C_f}\right) * \sqrt{\frac{\pi}{2} * \left(\frac{C_f}{C_{in} + C_j + C_f}\right) * f_{GBW}} \quad (10)$$

$$N_{Voltage} = 5.8\frac{nV}{\sqrt{Hz}}\left(\frac{27.6pF}{15.52pF}\right) * \sqrt{\frac{\pi}{2} * \left(\frac{15.52pF}{27.6pF}\right) * 2.01\,MHz} = 9.69\,\mu Vrms$$

Then, the total noise (N_{tot}) of TIA can be calculated using Eq. 11 which is a root-sum-square (RSS). Then the result of that calculation is the total noise value of the circuit is 0.19 µVrms on target f_{GBW} of 1 MHz.

$$N_{Total} = \sqrt{N_{Rf}^2 + N_{current}^2 + N_{voltage}^2} \quad (11)$$

$$N_{Total} = \sqrt{(16.28\,\mu Vrms)^2 + (0.11\,\mu Vrms)^2 + (9.69\,\mu Vrms)^2} = 0.19\,\mu Vrms$$

The plot of the f_{GBW} from 1 MHz to 10 MHz is shown in Figure 3. The plot shows that the noise value is linear with the f_{GBW}.

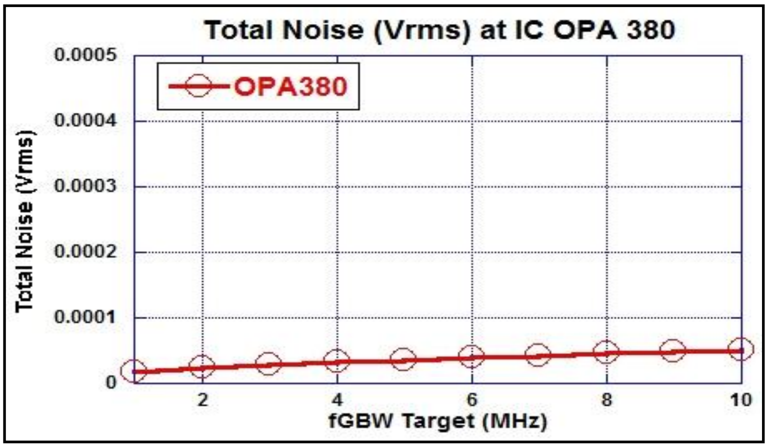

Figure 3. Total noise (µVrms) vs f_{GBW} (MHz) of Op-Amp OPA380 with C_j = 11 pF, C_f = 15.52 pF & R_f = 8 kΩ based on mathematical calculation

This experiment use component C_f and R_f with value as calculated before, *i.e* 15.52 pF and 8 kΩ, but the commercially available component for capacitor and resistor with the nearest value is 15 pF for the C_f and 8.2 kΩ for R_f. Table 2 contains the comparison of the ideal component with value as calculation and commercially available component, with double-digit precision after the decimal point. This comparison shows the difference between case I and case II is insignificant, so further analysis can be done using ideal value.

Table 2. Comparison of ideal component and commercially available component, GBW = 1 MHz & C_j =11 pF

Variable	Ctot (pF)	f -3db (MHz)	ENBW (MHz)	Noise Rf (µVrms)	Noise current (µVrms)	Noise voltage (µVrms)	Noise total calculation (µVrms)	Noise total simulation (µVrms)
Rf = 8 kΩ, Cf = 15.52 pF **(ideal)**	27.61	1.28	2.01	16.28	0.11	9.69	18.94	10.28
Rf = 8.2 kΩ, Cf = 15 pF **(case I)**	27.10	1.27	1.99	16.38	0.11	9.77	19.07	10.42
Rf = 8.2 kΩ, Cf = 22 pF **(case II)**	34.10	1.27	1.99	16.38	0.11	9.05	18.71	9.73

3.4. Simulation

Figure 4 is the TINA-TI™ simulation schematic of the TIA circuit. The current source of the photodiodes (I_{G1}) is components model for the SFH213 Si Photodiode and capacitor with 27.619 pF is the equivalent capacitor of C_{tot}. The OPA380, which is supplied by dual power supply 5 $V_{DC,}$ is available in the simulator. Next step is to click 'Analysis' menu and choose "AC analysis" then "AC transfer characteristic". Choose start frequency from 1 Hz to 10.5 MHz, then gain of the circuit will be shown, which is 78.06 dB then if reduced by three (f_{-3dB}), the value of point 'x' will be 1.3 MHz. Then, on the phase margin, 1.3 MHz point is perpendicular with 47.17^o, reduced by 1.22^o resulted in 46.24^o phase margin. This simulation result can be seen in Figure 5. The Bode plot comparison between calculation and simulation is shown in Table 3.

For the noise analysis (Figure 6), on the TINA simulator, choose "Analysis" menu then click "Noise Analysis". Choose start frequency from 0.5 MHz to 10.5 MHz, the number of points = 1000. Based on the simulation, the noise was measured and have different average of 2.2 µVrms (shown in Table 4) with the calculated value. This difference is because the simulation uses different approach, but the difference is relatively small and can be ignored.

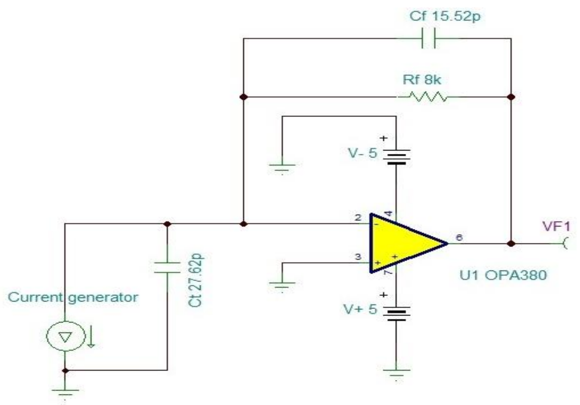

Figure 4. TIA circuit based simulation using offline TINA-TI™ with C_{tot} = 27.62 pF and ideal components: C_f = 15.52 pF & R_f = 8 kΩ

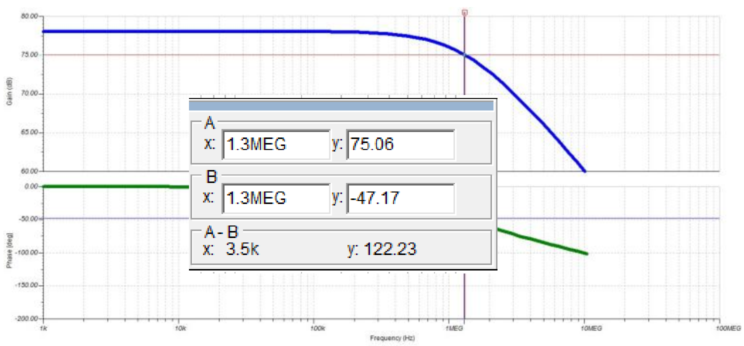

Figure 5. Bode plot and loop gain of the TIA; x(A) = frequency in MHz & y(A) = Gain in dB; x(A) = frequency in MHz & y(A) = phase margin

Table 3. Comparison of the f_{-3dB} and phase margin between ideal calculation and simulation

Variable	Calculation	Simulation
Cut-off frequency	1.28 MHz	1.30 MHz
Phase margin	45^o	46.24^o

Table 4. Noise comparison between simulation and calculation results

f_{GBW}	Calculation (µVrms)	Simulation (µVrms)	Error
1 MHz	18.94	10.28	8.66
2 MHz	24.43	18.85	5.58
3 MHz	28.83	25.16	3.67
4 MHz	32.72	30.38	2.34
5 MHz	36.3	34.89	1.41
6 MHz	39.64	38.9	0.74
7 MHz	42.81	42.54	0.27
8 MHz	45.87	45.88	-0.01
9 MHz	48.80	48.97	-0.17
10 MHz	51.65	51.86	-0.21

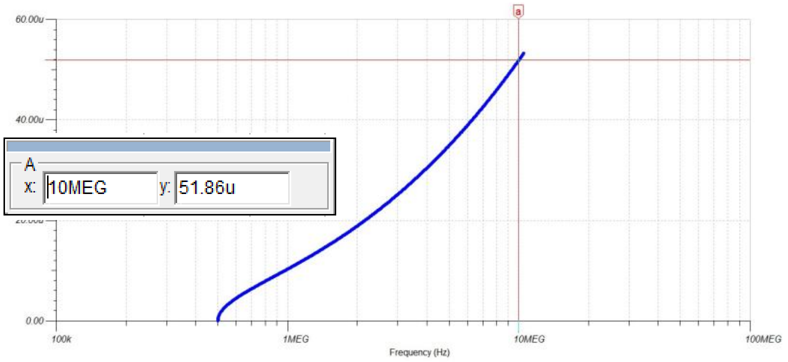

Figure 6. Total noise (µVrms) vs f_{GBW} (MHz) in Op-Amp OPA380 with C_j = 11 pF, C_f = 15.52 pF & R_f = 8 kΩ based simulation using offline TINA-TI™; x(A) = frequency in MHz & y(A) = total noise in micro scale

3.5. Final Prototype

The printed circuit board (PCB) is designed using PROTEUS 7.0, ISIS for schematic design and ARES for layout (Figure 7a). TIA kit is assembled on a single layer PCB with discrete components (Figure 7b) which consisted of one Op-Amp, one resistor feedback 0.25 Watt connected in parallel with capacitor feedback, 5 output pin (data, ground, supply-, ground, supply+), input pin from photodiode, two channels to tap in, and dual-supply pin with 5 V_{DC}. The OPA380 is SOIC8 fabricated IC because this kit is designed to use DIP type, PCB converter from SOIC8 to DIP needs to be used. The size of this TIA kit is 28.37 mm x 38.55 mm.

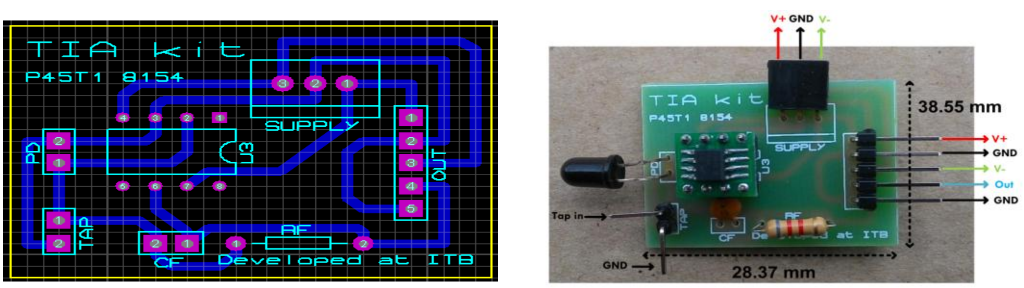

(a) (b)

Figure 7. Final prototype: (a) PCB layout; (b) A photograph of TIA kit

4. Conclusion

Based on the theories, VLC can offer high-speed data transfer (up to GHz scale) and large bandwidth which is more than Radio Frequency (RF) and other optical wireless technology such as infra-red communication (IR). Although, in reality, VLC system has a limitation on the component devices such as in the digital signal processing (DSP) system and in the analog front-end (AFE). Many solutions are offered to tackle that problem, one of the solutions is optimization of transmitter and receiver module on the analog system domain. The common problems of the AFE are in the active component selection, *i.e.* Op-Amp, with high bandwidth and low noise specification. In this paper, TIA design for low internal noise has been discussed. Using calculation and simulation approach, the designed TIA kit able to have low noise and low impedance characteristic.

Through this noise analysis, we hope that precise component selection can be done. Because this experiment is focusing more on the noise, the bandwidth characteristic is not much discussed. On the next research, the authors will compare the calculation and simulation results with real measurements, using tools for noise and bandwidth analysis of the TIA kit. To minimize the parasitic capacitances, the PCB design has to be done thoroughly. A double-sided glass epoxy with the surface mount devices (SMD) components is recommended, so that, the TIA circuit has optimum performances.

References

[1] Nakagawa Labolatories. Inc. [Online], Available at: http://www.naka-lab.jp/product/kit_e.html. Accessed in January 22, 2017.

[2] Disney Research Group. [Online], Available at: https://www.disneyresearch.com/project/visible-light-communication/. Accessed in January 22, 2017.

[3] PureLiFi. [Online] Available at: http://purelifi.com/. Accessed in January 22, 2017.

[4] OpenVLC. [Online], Available at: http://www.openvlc.org/. Accessed in January 22, 2017.

[5] A. Pradana, N. Ahmadi, and T. Adiono, *Design and Implementation of Visible Light Communication System using Pulse Width Modulation*. The 5th Int. Conf. on Electrical Engineering and Informatics (ICEEI), Bali. August 2015: 25-30.

[6] A. Pradana, N. Ahmadi, T. Adiono, W.A. Cahyadi, and Y-H. Chung. *VLC Physical Layer Design based on Pulse Modulation (PPM) for Stable Illumination*. Int. Symposium on Intelligent Signal Processing and Communication Systems (ISPACS). Bali. November 2015: 368-373.

[7] T. Adiono, A. Pradana, R.V.W. Putra, and S. Fuada. *Analog Filters Design in VLC Analog Front-End Receiver for Reducing Indoor Ambient Light Noise*. The IEEE Asia Pacific Conference on Circuit and Systems (APCCAS). Jeju. October 2016: 581-584. DOI: 10.1109/APCCAS.2016.7804058.

[8] S. Fuada, A.P. Putra, Y. Aska, and T. Adiono. *Trans-impedance Amplifier (TIA) Design for Visible Light Communication (VLC) using Commercially Available OP-AMP*. Proc. of the 3rd Int. Conf. on Information Tech. Computer, and Electrical Engineering (ICITACEE), pp. 31-35, October 2016. DOI: 10.1109/ICITACEE.2016.7892405.

[9] S. Fuada, T. Adiono, A. P. Putra, and Y. Aska. *A Low-cost Analog Front-End (AFE) Transmitter Designs for OFDM Visible Light Communications*. Proc. of the IEEE Int. Symposium on Electronics and Smart Devices (ISESD), pp. 371-375, March 2017. DOI: 10.1109/ISESD.2016.7886750.

[10] A.P. Putra, S. Fuada, Y. Aska, and T. Adiono. *System-on-Chip Architecture for High-Speed Data Acquisition in Visible Light Communication System*. Proc. of the IEEE Int. Symposium on Electronics and Smart Devices (ISESD), pp. 63-67, March 2017. DOI: 10.1109/ISESD.2016.7886693

[11] T. Adiono, S. Fuada, A.P. Putra, and Y. Aska. Desain Awal *Analog Front-End Optical Transceiver* untuk aplikasi *Visible Light Communication*. J. Nasional Teknik Elektro dan Teknologi Informasi (JNTETI). November 2016; 5(4): 319-327. DOI: 10.22146/jnteti.v5i4.280.

[12] T. Adiono, Yulian Y. Aska, A.A. Purwita, S. Fuada, and A.P. Putra. *Modeling OFDM system with Viterbi Decoder Based Visible Light Communication*. Proc. of the Int. Conf. on Electronic, Information and Communication (ICEIC), January 2017.

[13] T. Adiono and S. Fuada. *Optical Interference Noise Filtering over Visible Light Communication System Utilizing Analog High-Pass Filter Circuit*. The 2017 Int. Symp. on Nonlinear Theory and Its Applications (NOLTA2017). Cancun, Mexico. December 2017.

[14] S. Fuada, A.P. Putra, Y. Aska and T. Adiono. *A First Approach to Design Mobility Function and Noise Filter in VLC System Utilizing Low-cost Analog Circuits*. Int. J. of Recent Contributions from Engineering, Science, and IT (iJES), Vol. 5(2), pp. 14 – 30, 2017. DOI: 10.3991/ijes.v5i2.6700.

[15] S. Fuada, T. Adiono, A. P. Putra, and Y. Aska. *LED Driver Design for Indoor Lighting and Low-rate Data Transmission Purpose*. Unpublished.

[16] S. Fuada, A.P. Putra, and T. Adiono. *Analysis of Received Power Characteristics of Commercial Photodiodes in Indoor LOS Channel Visible Light Communication*. Int. J. of Advanced Computer Science and Applications (IJACSA), Vol. 8(7), July 2017. DOI: 10.14569/IJACSA.2017.080722.

[17] S. Fuada, A.P. Putra, Y. Aska, and T. Adiono. *Short-range Audio Transfer through 3 Watt White LED based on LOS channels*. Int. Symp. on Intellegent Signal Processing and Communication Systems (ISPACS). Xiamen, China, November 2017.

[18] Y-H. Kim and Y-H. Chung. *Experimental outdoor visible light data communication system using differential decision threshold with optical and color filters*. SPIE Optical Engineering 54(4): 040501. April 2015.

[19] D.R. Dhatchayeny, A. Sewaiwar, S.V. Tiwari, and Y-H. Chung. *EEG Biomedical Signal Transmission using Visible Light Communication*. Proc. of Int. Conf. on Industrial Instrumentation and Control (ICIC). Pune. May 2015: 243-246.

[20] M. S. Islim and H. Haas. *Augmenting the spectral efficiency of enhanced PAM-DMT-based optical wireless communications*. Optics Express. 2016; 24(11): 11932-11949.

[21] E. Sarbazi, M. Safari and H. Haas*. Photon Detection Characteristics and Error Performance of SPAD Array Optical Receivers*. Proc. of the 4th Int. Workshop on Optical Wireless Communications (IWOW). Istanbul. 2015: 132-136.

[22] Z. Wang, C. Yu, W-D. Zhong, and J. Chen. *Performance improvement by tilting receiver plane in M-QAM OFDM visible light communications*. Optics Express**.** 2011; 19(14): 13418-13427.

[23] Y. Zhao and J. Vongkulbhisal. *Design of Visible Light Communication Receiver for On-Off Keying Modulation by Adaptive Minimum-Voltage Cancelation*. Engineering Journal. 2013; 17(4): 125-129.

[24] M. S. Rahman, M. Haque, and K-D. Kim. *Indoor Positioning by LED Visible Light Communication and Image Sensors.* Int. J. of Electrical and Computer Engineering (IJECE). 2011; 1(2): 161.170.

[25] S. Gayatri and D. Bhalerao. *Comparitson of Different modulation techniques for high bandwidth visible light communication*. Int. Conf. on Electrical, Electronics, Signal, Communication and Optimization (EESCO). Andhara Pradesh. 2015: 1-5.

[26] H. Li, X. Chen, B. Huang, D. Tang, and H. Chen. *High Bandwidth Visible Light Communications Based on a Post-Equalization Circuit*. IEEE Photonics Technology Letters. January 2015; 26(2): 119-122.

[27] S. Fuada, A.P. Putra, Y. Aska, and T. Adiono. *Noise Analysis of Trans-impedance Amplifier (TIA) in Variety Op Amp for use in Visible Light Communication (VLC) System*. Int. J. of Electrical and Computer Engineering (IJECE).

[28] S. Verma, A. Shandilya, and A. Singh. *A model for reducing the effect of ambient light source in VLC system*. Proc. IEEE Int. Advance Computing Conf. Bangalore. 2014: 186-188.

[29] T. Adiono, R.V.W. Putra, and S. Fuada. *Noise and Bandwidth Considerations in Designing Op-Amp Based Transimpedance Amplifier for VLC*. Unpublished.

[30] L. Orozco. *Optimizing Precision Photodiode Sensor Circuit Design*. [Online], Available at http://www.analog.com/media/en/technical-documentation/technical-articles/Optimizing-Precision-Photodiode-Sensor-Circuit-Design-MS-2624.pdf. Accessed in January 23, 2017.

[31] Y.K. Law. Design and Testing of Off-The-Shelf Electronic Components for an Acoustic Emission Structural Health Monitoring System Using Piezoelectric Sensors. M.Sc Thesis. Virginia: Mechanical Engineering of the Virginia Polytechnic Institute and State University; August, 2005.